JOURNAL GEOLOGICAL SOCIETY OF INDIA
Vol.97, September 2021, pp.1087-1096

Role of Climate and Topography on Hydrological Characteristics of the Bharathapuzha Basin in the Tectonically Quiescent Western Ghats, India

S. Kiran Kumar Reddy[1], Sravan Kumar Kotluri[1], Harish Gupta[2*] and D. Venkat Reddy[1]

[1]CSIR-National Geophysical Research Institute, Hyderabad - 500 007, India

[2]Department of Civil Engineering, Osmania University, Hyderabad - 500 007, India

**E-mail: harishgupta78@osmania.ac.in*

ABSTRACT

Intra-basin variations in sediment supply provide clues for understanding the erosion process and the role of local topographic features and climatic factors. Hence in this study, Bharathapuzha (BP) basin from tectonically quiescent Western Ghats (WG) was selected to examine the role of topography and climate on the sediment erosion process across its sub-basins. Multi-years daily water discharge and sediment load data of five monitoring stations were combined with morphometric parameters to visualize the local variability in sediment erosion rates. The average annual water discharge and sediment load of the BP basin to the Arabian Sea are 4.71 km^3 and 0.37×10^6 tons. Interestingly, Kunthipuzha (KP) sub-basin, despite covering 17% of the total basin area, contributes around 41% and 27% of water discharge and sediment flux, respectively. The sediment yield (erosion rate) from the KP sub-basin is ten times higher than the same sized sub-basin within the BP catchment. For comprehending the role of topography and climate on these local variations, geomorphic indices such as Hypsometric integral (HI) and stream length (SL) index were calculated for the BP basin and sub-basins. Further, multiple regression was used to explore the quantitative relationships among the influencing factors. Results suggest that the rainfall and topography critically influenced basin erosion and explained 93% of the total variance. This study demonstrates the importance of intra-basin scale processes even for small mountainous rivers and signifies the role of local variations in topography and climate in erosion and material transport.

INTRODUCTION

Rivers are the prime pathways to deliver freshwater and suspended sediment to the coastal regions (Milliman and Meade 1983, Milliman and Syvitski 1992). Small scale mountainous rivers received little and late attention from the scientific community. However, the subsequent studies have attempted to fill this gap (Milliman and Syvitski 1992; Farnsworth and Milliman 2003; Kao and Milliman 2008). The rivers draining from the young mountains of southeast Asia and Oceania having catchment areas smaller than 10^3 km^2 alone contribute approximately 40% of the sediment reaching the global ocean (Milliman et al. 1999). Most of these rivers are draining through the tectonically active continental margins, and extreme (episodic) events occur in <1% of the time contribute to >75% of the long term sediment flux (Kao and Milliman 2008). Tectonics, bedrocks, basin morphology, and human activities are the dominant factors for this disproportionate amount of freshwater and sediment delivery from these watersheds (Dadson et al. 2003; Hilton et al. 2008). In contrast, a limited number of studies have investigated the factors controlling the water and sediment delivery from the passive mountain regions.

The fluvial channel network represents relationships between relief, elevation, and erosion rates and conveys quantitative temporal information on tectonic and climate forcing across the landscape (Wobus et al. 2006; Jaiswara et al. 2019). Besides the climate and lithology, the morphology of a basin is an essential parameter to explain the denudation rates and resultant sediment load (Ruxton and McDougall 1967). Quantitative measurements such as geomorphic indices are frequently used to investigate basin deformation, erosional and evolutional status of drainage basins on a regional scale (Keller 1986; Keller and Pinter 2002; Peters and van Balen 2007; Stepancikova et al. 2008; Shi et al. 2020). The advancement of tools and availability of high-resolution data products facilitated the scientific community to investigate the roles of tectonics and climate on landscape evolution using geomorphic indices. Widely used and well known geomorphic indices include hypsometric integral and stream length gradient index. These geomorphic indices provide clues about the state of the river basin in terms of its stability and erodibility (Lifton and Chase 1992; Chen et al. 2003; Kale and Vaidyanadhan 2014). Therefore, a better understanding of the relationship between erosion rate and its potential influencing factors is essential to improve the understanding of the fluvial geomorphology of a region.

Peninsular India as part of the Gondwana, experienced a series of significant rifting events that led to its eventual break-up during the Mesozoic period and became tectonically quiescent after that (Storey 1995; Chatterjee et al. 2013). During the late Cretaceous period, the western margin of Peninsular India was rifted successively from Madagascar (Storey et al. 1995; Torsvik et al. 2000; Gunnell et al. 2003) and Seychelles Bank (ca. 65 Ma; Hooper 1990; Collier et al. 2008; Minshull et al. 2008). Subsequently, it became the passive margin of the Arabian Sea. Thus, the Western Ghats (WG) escarpment has been recognized as a rift shoulder and being reshaped by post-rifting erosional processes (Campanile et al. 2008; Gunnell and Harbor 2010) and extends from the Satpura range in the north to the Anamalai in the south. Morphologically, the WG consists of a 30-80 km broad, low-lying coastal strip, divided from an elevated inland plateau by a steep continuous escarpment from 8° N to 20° N latitude. It has been acting as a host for many large east-flowing rivers and numerous small west-flowing rivers (Kale and Vaidyanadhan 2014). Tectonics, climate change, and the Indian plate movement affected the east-flowing rivers, whereas climate change is the primary control affecting the west-flowing rivers (Kale and Rajaguru 1988). The WG escarpment evolved during ~65 Ma (Keller, 1986) as an elevated passive continental margin in the west coast of the Indian peninsula has become host to several small mountainous rivers (Guha and Jain 2020; Reddy et al. 2021). These small mountainous rivers drain the western flank of the Western Ghats primarily and receive copious rainfall from the southwest (SW) monsoon between June and September (Gunnell and Bourgeon 1997;

0016-7622/2021-97-9-1087/$ 1.00 © GEOL. SOC. INDIA | DOI: 10.1007/s12594-021-1824-x

Padmalal et al. 2018). Studies by Radhakrishna (1964), Dikshit (2001), Ambili and Narayana (2014) investigated the form and structure of drainage for the west-flowing drainage basins. However, the role of climate and topography on the sediment yield (erosion rate) is yet to be investigated. Except for a ~30 km wide major topographic break called 'Palghat Gap', the WG is a continuous mountain chain and acts as a climate barrier for summer monsoon (Gunnell 1997; Mandal et al. 2017). The Bharathapuzha (BP) river traverses through the central part of the Palghat gap and is an attractive avenue for researchers. The sub-basins of the BP show substantial variability in topography and climatic parameters; hence, it might be influencing the hydrological processes. Therefore, the objectives of the current study are to (i) investigate the variability in runoff and sediment yields across the sub-basins; and (ii) look into the relative roles of climate, topography, and lithology as the driver to hydrological characteristics of sub-basins.

STUDY AREA

The WG region is drained by over 600 small mountainous rivers characterized by a steep westerly gradient created a huge fluvial network and associated sediment accumulation on the west coast (Radhakrishna 1994; Kale 2009; Reddy et al. 2021). The WG is divided into three major geo-tectonic units, Deccan Traps at the northern part, western Dharwar craton in the central part, and southern granulite terrain (SGT), also known as Pandyan Mobile Belt in the southern part. SGT consists of massive charnockite with mafic granulite (Ghosh et al. 2004; Reddy et al. 2019). The present study basin lies in the SGT region and passing through the 'Palghat Gap' at 11° N latitude by a ~30 km broad low relief, which is the widest topographic break across the WG (Fig.1).

The BP river originates in the Anamalai hills (1964 m), occupying 6,186 km^2 of the catchment area and with 209 km length, is the largest west-flowing river in the SGT (Reddy et al. 2019). Topographically, a small region of the BP basin is having the highlands landscape (>2000 m), followed by the lowlands in the rest of the basin. The BP river has two major tributaries in the upper reaches which together forms a major sub-basin (Aliyar river; 2775 km^2). The other two tributaries, namely Gayatripuzha (1057 km^2) and Kunthipuzha (940 km^2), originate at either side of the mountainous region of the Palghat gap (Fig. 2a). The Kunthipuzha river originates in the northern

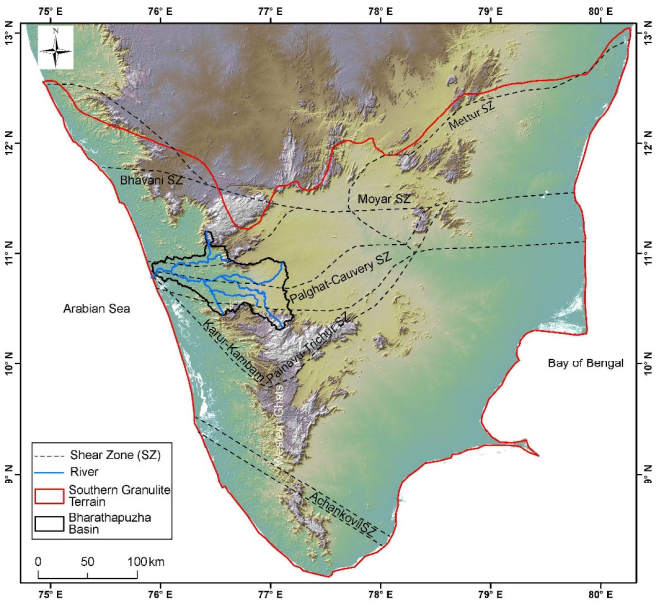

Fig.1. Map shows the structural features of the Southern Granulite Terrain (SGT).

mountainous part and drains through less disturbed evergreen forests of the Silent valley National Park before joining the mainstream (Magesh et al. 2013).

Geologically, the catchment of the BP consists of high-grade metamorphic rocks (granulite-amphibolite facies) of Archaean age belonging to the SGT (Ghosh et al. 2004; Chetty and Rao 2006). The lithology of the BP basin is dominated by Archaean crystalline rocks such as migmatites, charnockites, and garnet-sillimanite gneisses in the upper and midlands (Fig. 2b). Quaternary sediments, alluvium (locally Kankar formations) cover the coastal plains in low lands (Ramkumar et al. 2019), and laterites (Widdowson and Gunnell 1999; Fig. 2b). Structurally, the Palghat-Cauvery shear zone traversing through the SGT, Moyar, Bhavani, Palghat-Cauvery, and Attur shear zones are the major structural feature in south India (Fig. 1; Chetty and Rao 2006; Collins et al. 2007). Earlier studies have indicated that the Palghat Gap is structurally controlled as it coincides with the Palghat–Cauvery dextral shear zone (Chardon et al. 2008; Chetty and Rao 2006).

The WG acts as a climatic barrier to the southwest winds and results in deep convection that contributes to heavy orographic rainfall on the coastal plains and over the foothills (Grossman and Durran 1984; Gunnell 1997). Therefore, from early May to September, the SW monsoon is the principal source of rainfall in most of the basin. On the other hand, the Palghat gap of the WG favours the domination of the NE monsoon from October to December in some of the eastern parts of the BP basin (Padmalal et al. 2018). The mean annual rainfall of the BP basin (Bookhagen and Burbank 2006;1751 mm) derived from Tropical Rainfall Measuring Mission is comparable to the reported monthly rainfall data of 34 years (1968–2002) from 29 rain gauge stations (Raj and Azeez 2012; 1828 mm). The temperature range in the basin varies from 22.7 °C (mean annual minimum) to 32.5 °C (mean annual maximum), with an average temperature of 27.5 °C (Reddy et al. 2019).

DATA AND METHODOLOGY

The Central Water Commission (CWC) of India maintains five gauge-discharge (GD) sites in the BP basin. Among these, three sites, i.e. Ambarampalayam (GD-1), Pudur (GD-2), and Mankara (GD-3) are located in the Aliyar sub-basin, and Pulamanthole (GD-4) is located in the Kunthipuzha sub-basin, whereas Gayatripuzha sub-basin has no GD site. Kumbidi (GD-5) on the mainstream is the terminal site for the entire BP basin (Fig. 2a). For the convenience of readers, the following acronyms were followed to sub-basins as Aliyar-AR, Gayatripuzha-GP, and Kunthipuzha-KP throughout the text. Hydrological characteristics of the GD sites and sub-basins for the present study are summarized in Table.1. In the present study, the discharge and suspended sediment data was acquired from five established GD sites covering the mainstream and sub-basins (Fig. 2a) from the WRIS-India portal (http://www.india-wris.nrsc.gov.in/) and the published reports of CWC for 1978-79 to 2016-17 (http://www.cwc.gov.in/wateryear-book). Due to significant seasonal variation in the rainfall of India, CWC measures the sediment load daily in the monsoon (SW) season and once in a week during the post-monsoon season. Procedures and techniques related to the discharge and sediment load estimations documented by CWC in annual reports and can also be referred from Gupta et al. (2012). Water discharge and sediment loads of respective GD sites were calculated using CWC data. Inverse distance weighting technique is applied to calculate the fluxes of the entire basin on the ArcGIS platform (Reddy et al. 2019).

In conjunction with discharge and suspended sediment data, drainage morphometry was analyzed to understand the erosion process and to evaluate the role of topography across the basin. Drainage basin morphometry provides a quantitative characterization of

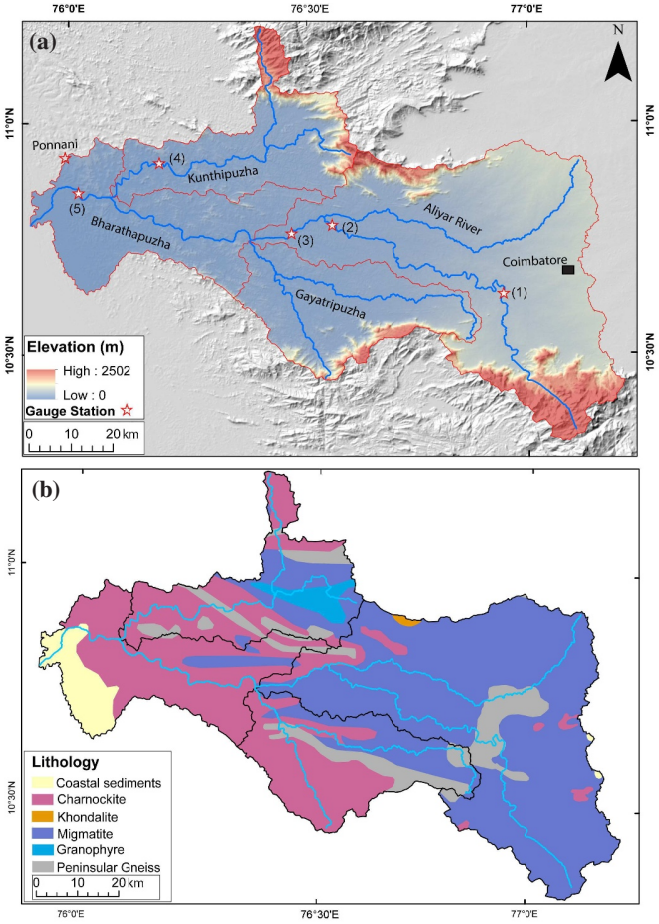

Fig. 2. (a) Location map of the Bharathapuzha river basin, showing the distribution of gauge-discharge (GD) sites across the sub-basins: Ambarampalayam (GD-1), Pudur (GD-2), Mankara (GD-3), Pulamanthole (GD-4) and Kumbidi (GD-5); **(b)** Geology/lithology of the Bharathapuzha River basin (Modified after GSI1995).

basin morphology by identifying variations in the spatial and linear attributes of a drainage basin and helps in characterizing the stages of erosion in comparison to the basins of varying topographic relief (Keller and Pinter 2002; Bull 2007; Anderson and Anderson 2010; Burbank and Anderson 2011). The hypsometry and SL index are basic tools (Strahler 1952; Hack 1973) for any morphometric analysis that broadly defines river basin evolution stages (i.e. young, mature, old). They help to identify the zones of localized erosion based on stream gradient along with the profiles. Understanding the evolutionary stage of sub-basins in response to discharge and suspended sediment, the hypsometric curves and SL-index along with river profiles, were carried out using ArcGIS and MATLAB programs (Jaiswara et al. 2020). The basin's geomorphic indices are extracted from the 90-m spatial resolution of the Shuttle Radar Topography Mission-Digital Elevation Model (SRTM-DEM; http://srtm.csi.cgiar.org/; Jarvis et al. 2008). The drainage network has been extracted by using the D8 algorithm (O'Callaghan and Mark 1984; Fig.2a).

The hypsometric (area-altitude) curve is a function of the cumulative area (a/A) and the cumulative height (h/H), where a is surface area within the contour, A is the total drainage basin area, h is the height of the basin within the contour, the total height H is the relief within the basin, and the axes are scaled from 0 to 1 (Strahler 1952). These curves are quantified in the form of the hypsometric integral (HI). The area below the hypsometric curve represents the un-eroded volume of the basin and is calculated as

$$\text{Hypsometric integral (HI)} = E_{mean} - E_{min} / E_{max} - E_{min}$$

where, E_{min}, E_{mean} and E_{max} are the minima, mean and maximum elevation of the drainage basin. The shape of the hypsometric curve defines the evolutionary stage of the channel and is used to assess the erosional process of the landscape (Strahler, 1952).

Bedrock river profiles tend to maintain the steady-state between tectonics and erosion (Schumm et al. 2002; Keller and Pinter 2002). Derivation of the river profile is called Stream Length (SL) index, which is derived using the following equation

$$\text{Stream length Index (SL)} = \Delta H/\Delta L * L$$

Where L is the total length of the channel from the water divide, ΔH is the drop in elevation, and ΔL is the length of the local reach (ΔL=5 km in the present study) for which the index is calculated. SL-index profiles have been extracted and plotted along with the river profiles for the channels of the Bharathapuzha basin to understand the erosion process.

RESULTS

Water discharge and sediment flux of a basin and its sub-basins reflect the type and intensity of the hydrological process. Sediment erosion rates (denudation rates) being neutral to the size of catchments allow comparing the intensity of the erosion process in different sub-catchments. Therefore, to understand these processes, in the first part of this section, results on the spatial variability in hydrological parameters such as water discharge and sediment load and yields of five GD sites are discussed. The results of morphological investigations are described in the subsequent section. It is complemented by investigation through geomorphic indices of sub-basins and the entire basin, which offers information on the geomorphic evolution and erosion stage.

Discharge and Sediment Flux

The daily sediment load (Y1-axis) of the five GD stations from 1st June-2017 to 31st May-2018 (a representative water year of CWC) mimic the corresponding daily discharge patterns (Fig. 3a-e). However, spatial variability is visible across the sites in patterns and order of fluxes. Among the 5 GD sites, daily water discharge and sediment flux are lowest at the upstream site (Ambarampalayam) of the AR sub-basin (Fig. 3a). Due to the upstream flow contribution, a gradual increase in daily water discharge and sediment flux from Ambarampalayam to Mankara is observed in the AR sub-basin (Fig. 3a to c). Daily water discharge and sediment flux of the KP river draining the northern side of the BP basin at the Pulamanthole GD site is remarkably higher than the AR sub-basin (Fig. 3d). The time-series daily discharge and sediment flux data of the corresponding GD sites (Table 1) is used to estimate the mean monthly values for the AR, KP, and the BP basin (Fig. 3f to j). A single peak in water discharge and sediment flux at Ambarampalayam (Fig. 3f) is observed during November-December (NE monsoon). The percentage contribution of water discharge and sediment flux during SW and NE monsoon seasons at the Ambarampalayam site is 28 & 42% and 29 & 46%, respectively (Table 1). In contrast to the uni-modal pattern at Ambarampalayam, it is a bi-modal pattern in water discharge and sediment flux at the Pudur and Mankara GD sites. It is surprising as all these three sites, being part of the AR sub-catchment, show different discharge patterns. Although both the sites are showing the bimodal pattern in the mean discharge and sediment flux, the influence of NE monsoon is great (35% & 16%) at Pudur compared to Mankara (29% & 11%) (Fig. 3 g, h; Table 1). Overall, the influence of SW and NE monsoon is visible through uni-modal and bimodal discharge patterns (Fig. 3e, f & g) within a small sub-catchment (<3000 km^2).

The other GD sites, Pulamanthole (KP sub-basin) and Kumbidi (BP basin) follow the uni-modal pattern with a high contribution of mean discharge and sediment flux during the SW monsoon season

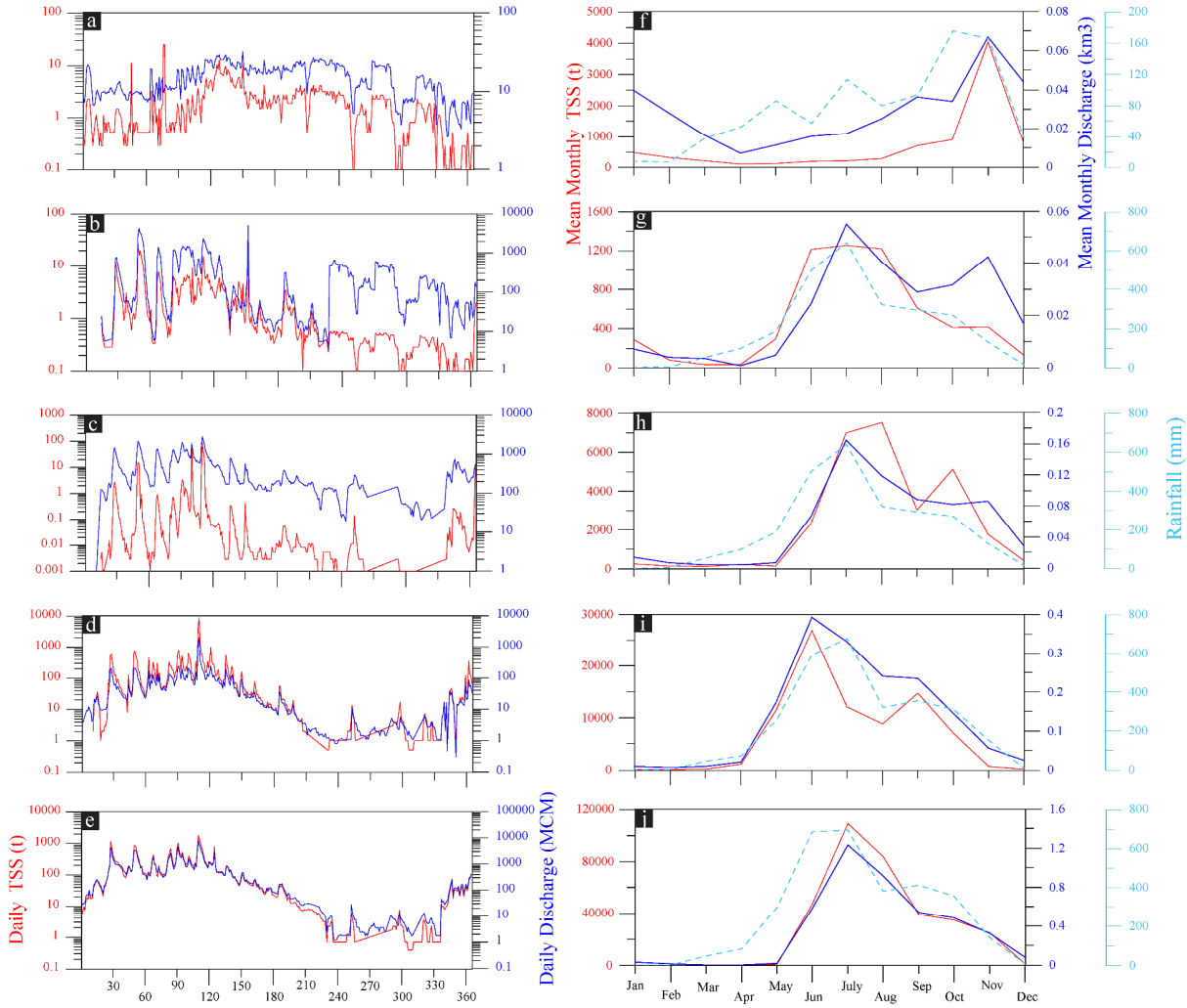

Fig.3. Daily and mean monthly rainfall, discharge, and sediment flux at five gauge sites of the Bharathapuzha basin. (Note: TSS indicates the Total Suspended Sediment).

(Table 1). It indicates the dominance of the SW monsoon season in the lower reaches of the BP basin (Fig. 3 i & j). Similar patterns in discharge and sediment flux are also observed by Padmalal et al. (2018) for the BP basin. The monthly mean of the discharge and sediment flux generally follow the rainfall pattern for the BP catchment. It implies that the variation in rainfall across the BP basin is the primary factor resulting in the spatial variation in discharge and sediment flux of the sub-catchments. Broadly, the discharge pattern advocates that the topographic gap (i.e. Palghat gap of the WG) connects the NE monsoon with the SW monsoon from upstream to downstream regions of the BP basin.

The mean annual discharge on the Ambarampalayam, Pudur, Mankara, Pulamanthole, and Kumbidi GD sites are 0.33, 0.27, 0.67, 1.73, and 4.22 km^3. It implies that the AR, KP, and BP rivers discharge is 0.67, 1.73, and 4.22 km^3, respectively. Despite draining the one-third area of the AR sub-basin, the discharge of the KP sub-basin is three times higher (Table 1). Significant variability in hydrological characteristics across the basin is evident from the annual runoff of the AR (259 mm), KP (1837 mm), and the BP (761 mm) basins. The mean annual sediment flux of the five sites are 0.008, 0.006, 0.028, 0.089, and 0.345 million tons (MT) for Ambarampalayam, Pudur, Mankara, Pulamanthole, and Kumbidi stations, respectively. The mean annual runoff of the KP sub-basin is three times higher than that of the entire BP basin and highest among the sub-basins (Table 1). Interestingly, despite draining one-third (940 km^2) area to the AR sub-basin (2775 km^2), the annual runoff (1837 mm) and sediment flux (0.089 MT) of the KP sub-basin is about three times higher than that of the AR basin (259 mm; 0.028 MT). The area normalized annual sediment flux (yield) of the Ambarampalayam, Pudur, Mankara, Pulamanthole, and Kumbidi GD sites are 8.9, 4.6, 10.1, 95.2, and 60.4 t km^{-2}, respectively. It implies that the intensity of sediment erosion at the KP basin is almost ten times higher than the AR basin (Table 1). Additionally, the sediment yield of the KP sub-basin (95.2 t km^{-2} yr^{-1}) is higher among the coastal rivers draining the SGT region (Reddy et al. 2021). High erosion rates in the KP sub-basin can be attributed to the presence of elevated topography and orographic effects.

The overall annual water discharge and sediment flux from the whole BP river to the Arabian sea is 4.71 km^3 and 0.37 MT, and the runoff and sediment yields are 761 mm and 60.4 t $km^{-2,}$ respectively (Table 1). These estimations are comparable to the previous estimations for the BP basin (Padmalal et al. 2018). Despite occupying 17% of the total BP basin area, the KP sub-basin alone contributes 41% and 26% of the total discharge and sediment flux (Table 1), respectively. The same is evidenced by the time-series annual loads of discharge and sediment flux from Pulamanthole (KP sub-basin) and Kumbidi (BP basin) sites (Table 1).

Geomorphic Analysis

The topographical relief map shows the dominance of low relief landform features across the basin (mean basin elevation-291 m), barring few exceptions (Fig. 4a). High relief rugged mountains are

Table 1. Hydrological parameters of Bharathapuzha basin and its sub-basins

GD location	River name	Basin area (km^2)	Latitude	Longitude	Discharge ($km^3\ yr^{-1}$)	Runoff ($mm\ yr^{-1}$)	Period (yr)	% Contribution			Sediment ($M.T\ yr^{-1}$)	Yield ($T\ km^{-2}\ yr^{-1}$)	Period (yr)	% Contribution		
								SW	NE	NM				SW	NE	NM
Ambarampalayam	Aliyar	950	10°37'49"N	76°56'46"E	0.36	377	1978-79 to 2016-17	28	42	30	0.008	8.88	2003-04 to 2016-17	46	25	29
Pudur		1313	10°51'00"N	76°01'12"E	0.28	212	1986-87 to 2016-17	57	35	8	0.006	4.57	2013-14 to 2016-17	72	16	12
Mankara		2775	10°45'40"N	76°29'10"E	0.72	259	1985-86 to 2016-17	65	29	5	0.028	10.14	2013-14 to 2016-17	74	11	15
Pulamanthole	Kunthipuzha	940	10°46'48"N	76°34'30"E	1.73	1837	1986-87 to 2016-17	73	14	13	0.089	95.21	1986-87 to 2016-17	75	9	16
Kumbidi	Bharathapuzha	5755	10°53'57"N	76°11'50"E	4.38	761	1980-81 to 2016-17	77	21	2	0.345	60.4	1980-81 to 2016-17	82	17	1
	Bharathapuzha Basin*	6186			4.71	761		77	21	2	0.37	60.4		82	17	1

Yield = Sediment yield (specific flux); GD= Gauge and Discharge; SW= Southwest monsoon; NE=Northeast monsoon; NM=Non-monsoon; *Total basin

restricted mainly to upstream areas of KP and GP sub-basins (Fig. 4a). Palghat Gap results in the upstream region of the BP basin experiencing a semi-arid climate, whereas the downstream region receives heavy downpour. The Palghat Gap facilitates the inward movement of monsoon winds, and due to the orographic effect of local topographic relief, these areas of the KP and GP sub-basins receive heavy rainfall. Locally, the mean annual rainfall of the KP sub-basin (~5600 mm) is highest, which is three times higher than the mean annual rainfall (1751 mm) of the entire BP catchment. This uneven distribution in mean annual rainfall is well reflected in Figure 4b. The latitudinal swath profile of the BP basin demonstrates the coupling of topography and rainfall (Fig. 4c), stressing the remarkable orographic effect of local relief features. The extracted geomorphic indices were analyzed and compared with the observed qualitative maps such as relief and rainfall of the BP basin to evaluate the role of climate and topography on the surface erosion rates.

The hypsometric curves (area-altitude curve) relates the horizontal cross-sectional area of a drainage basin to relative elevation above the basin mouth. It can be compared across basin and sub-basins to infer geomorphic evolution stages in response to changes in tectonic forcing or spatial variations of erosional processes or the development stages of a given drainage basin (Strahler 1952; Montgomery et al. 2001; Pérez-Peña et al. 2009, 2010). For understanding the basin evolution stage, hypsometric curves and indices have been calculated for the BP basin, all the sub-basins, and including the GP basin though it does not have the GD location on this river to measure the discharge and

Fig.4. Local variations in **(a)** basin topography **(b)** mean annual precipitation and **(c)** latitudinal swath profile demonstrating the coupling of topography and rainfall across the Bharathapuzha basin. 12-year average rainfall dataset of Bookhagen and Burbank (2006) is used for making spatial maps.

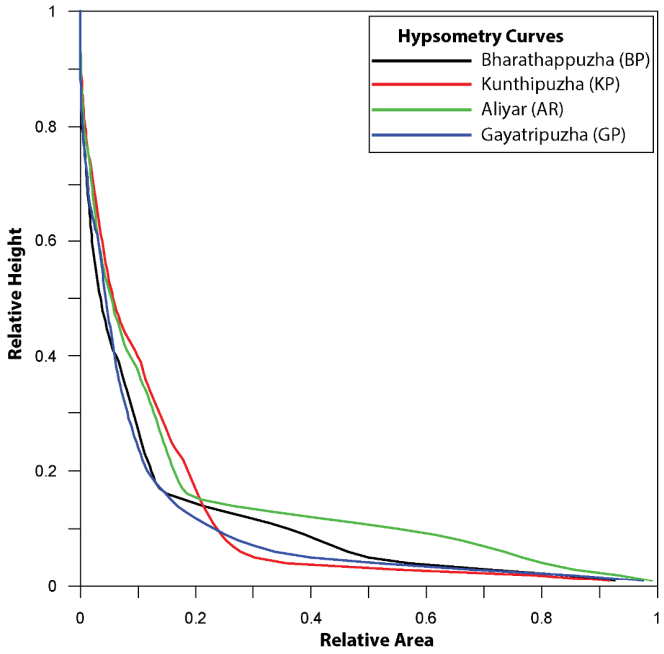

Fig. 5. Hypsometric curve indices for the Bharathapuzha mainstream and its tributaries

sediment load values. All the basins are displaying the concave-up curves with hypsometric integral (HI) values for the AR, GP, KP, and BP ranging 0.48, 0.46, 0.47, and 0.48, respectively (Fig. 5). Despite having different drainage areas and the presence of diverse topography landforms, the HI values of all sub-basins are comparable. It depicts that the topography effect on the small drainage basins of KP and GP is the same as their hypsometric values are comparable with large drainage area basins.

Rivers tend to maintain an erosion-sedimentation equilibrium or steady-state that is characterized by a concave longitudinal river profile, also known as river gradient profile (Schumm et al. 2002). The SL index defines the changes in stream slope, i.e. river gradient along with a longitudinal river profile, and effectively determines the zones of a topographic break. This sensitivity index allows the evaluation of relationships among possible tectonic activity, rock resistance, and topography. The SL-index can be correlated with stream power, and the total stream power available at a specific channel reach is an important hydrological variable. The SL-index relates to the ability of a stream to competence its bedrock and carry sediment (Hack 1973; Keller and Pinter 2002). The total power of the stream is proportional to the product of the slope and discharge of the water. The slope of the water surface is usually approximated by the slope of the channel bed (Keller and Pinter 2002). River profiles were extracted, the SL-index of AR, KP and GP (tributaries of BP) and BP was calculated, the trunk river to understand the variation of the stream power following the sediment discharge (Fig. 6). Among the tributaries, the KP river shows a concave profile and high stream power in the upper reaches indicated by the SL index, probably due to the high steepness of the topography (Fig. 6a). The GP river profile shows a gradient profile, which is almost in steady-state except in 80-100 km and 140-160 km reach segments, where the river is showing a little peak evidenced in SL-index (Fig. 6b). With low stream power, the AR river profile shows a gradient profile suggested by maximum SL-index values (250; Fig. 6c). The trunk profile of the BP shows convex up in the upper reaches; eventually, it became gentle in gradient (Fig. 6d).

DISCUSSION

The results presented in the previous section confirm remarkable variations in discharge and sediment flux. Most of the basin except the mouth of the river is overlain by crystalline rocks (Padmalal et al. 2018). Besides, it is found that erosion rates across the SGT region are comparable due to the dominance of uniform lithology (Guha and Jain 2020). It implies that the variability in sediment yields for small mountainous rivers of the WG might not be linked to limited lithological variability. This is in contrast to the small mountainous rivers of Taiwan and the Oceania (tectonically active) regions, where most of the rivers are flowing through sedimentary terrains (Milliman and Meade 1983; Liu et al. 2008). Lithology, which can actively regulate sediment flux, is not a prominent factor for this region. Therefore, the role of lithology in differential erosion is ruled out.

Due to the Palghat Gap, the basin receives rains in both the SW and NE monsoon seasons. However, due to the lack of high mountains

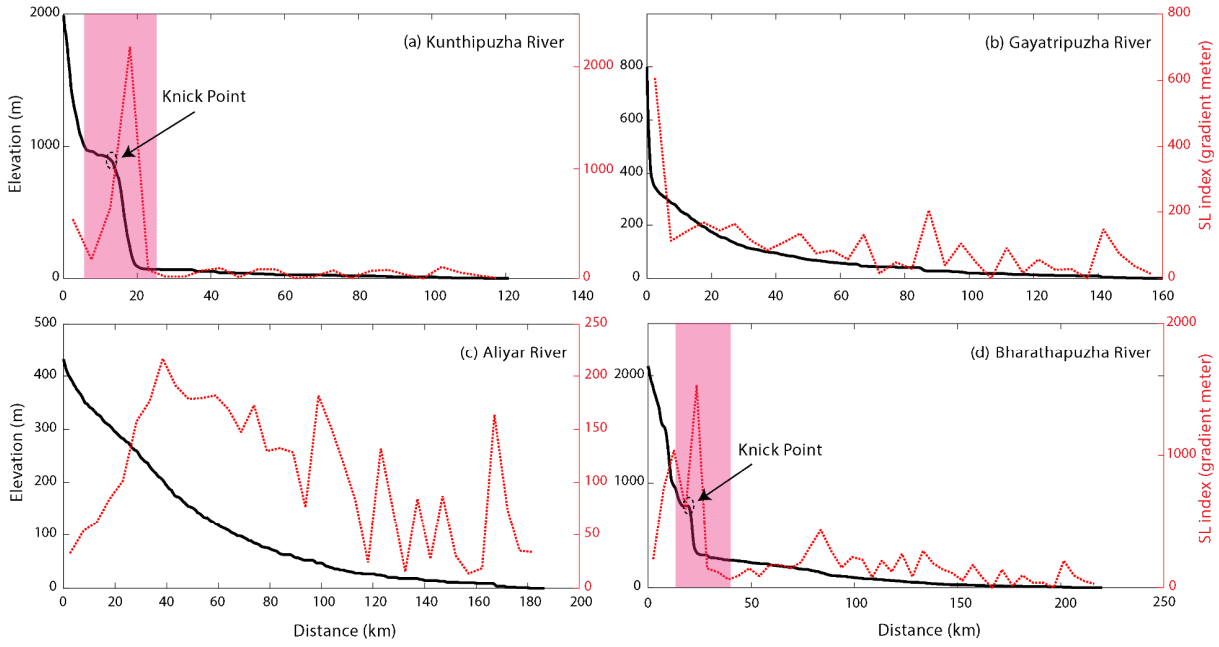

Fig. 6. River profiles of mainstream and tributaries and SL-index for the sub-basins and the BP basin

to intercept the NE monsoon winds, the upstream region experiences a semi-arid climate. Whereas northward moving SW monsoon is intercepted by mountains present in the KP sub-basin. This confirms that the BP basin is experiencing a non-uniform climate. In the western part, the climate is tropical monsoonal (Am of Koppen). It changes to Koppen's Aw (tropical savanna) towards the east, and at the eastern margin, the climate is semi-arid (Koppen's BS; Thrivikramji 1989). Mean annual runoff values across the BP basin vary by order (212-1837 mm) and indicate the climatic transformation from semi-arid to humid within the basin. In a recent study, Reddy et al. (2019) demonstrated that runoff is one of the dominant factors in the basin-scale weathering process in the west-flowing coastal rivers of the Indian peninsula.

Despite the dominance of low elevation landforms covering about 90% of the BP basin, it has a significant topography relief near drainage divides. The SL-index profiles display multiple topographic breaks in the upper reaches (Fig. 6). The steepest topographic regions stimulate the erosion process, especially in the areas of high precipitation. This impression is supported by the highest rates of runoff and sediment flux values in the KP sub-basin within the BP catchment. The denudation rate for the KP sub-basin (0.035 mm yr^{-1}) is almost double (0.022 mm yr^{-1}) that of the BP basin. The denudation rate of the AR basin (0.004 mm yr^{-1}) is extremely low to the basin average (0.022 mm yr^{-1}). Mandal et al. (2015) have documented the high denudation rates in the KP sub-basin using the measured Beryllium-10 (^{10}Be) concentrations in the whole SGT region despite its small catchment size. The present results support the findings of Mandal et al. (2015). Similarly, based on elevated topography and rainfall, a high erosion rate might be expected in the upper region of the GP sub-basin. Despite having similar lithology, the geomorphic indices, such as SL-index, vary substantially within the BP basin. The high topography relief and rainfall pattern upstream of the KP and GP sub-basins suggest that these regions are responsible for producing higher runoff and sediment flux in the BP catchment. On the other hand, the AR sub-basin flows in the Palghat Gap, and having low topography relief and receives little precipitation has meagre stream power reflected by SL-index (Fig. 6). Except in the southeast of the basin, the presence of a very low percentage of topography relief and low precipitation rate suggests that the AR basin might not have the capacity to produce high runoff and sediment flux. In contrast to this, the river profile and SL-index of the BP trunk channel is showing high stream power in the upper reaches. This is in line with the global displays of sediment yields reflect topography where the high yields equate to mountainous areas and low yields to lowlands (Walling and Webb 1996; Milliman and Meade 1983; Zhang et al. 2015). The low sediment flux rates at different GD sites of the basin are also supported by the presence of the concave hypsometric curves despite the large basin areas of the BP and AR river profiles.

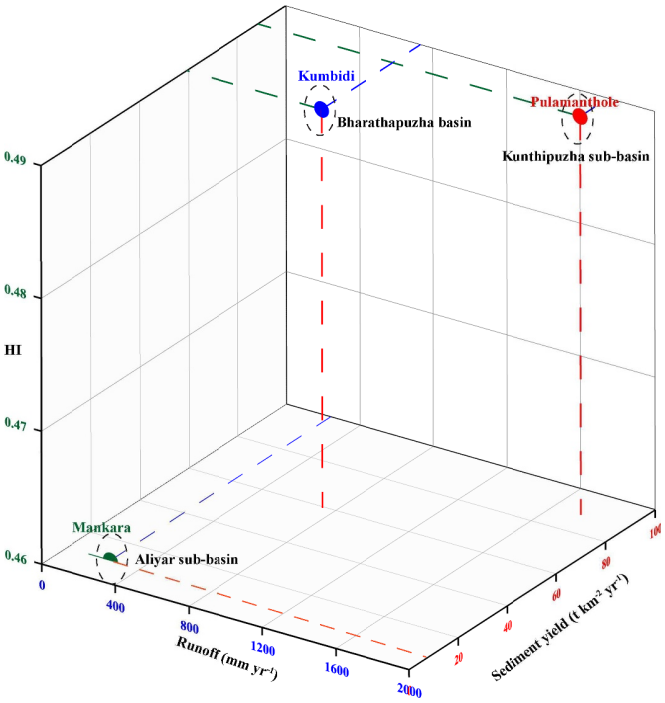

Fig. 7. Box plot showing the distribution of HI indices with respect to runoff and sediment yield for Gauge-Discharge sites of the river

The hypsometric curves from the BP basin and sub-basins indicate a mature stage, where all HI values are in the same order (~0.50); however, the patterns are dissimilar to each other. The concave shape of the AR sub-basin reflects the mature stage, where erosion is relatively low. The relative influence of HI and runoff on sediment erosion rates of different sub-basins and the BP basin is demonstrated in Fig.7. The AR sub-basin (Mankara) shows low runoff and low HI indices is characterized by low sediment yield. On the other side, the KP sub-basin (Pulamanthole) having a high runoff and HI, attributing to high sediment yield. It demonstrates that the erosion rate in the KP sub-basin is the highest among the sub-basins in the BP catchment. To better represent the combined role of topography and runoff, a multiple regression analysis was performed. Runoff and topography (HI) together explain 93% of the total variance in sediment yield.

A Pearson correlation (PC) analysis was performed on the other basin parameters (Data from Reddy et al. 2021) for the rivers draining from the SGT region (Table 2). PC analysis indicated that basin parameters such as catchment area, length of the river, and mean basin elevation has not shown any correlations with the sediment yield. Mean annual temperature showed a negative correlation (r=-0.48, p>0.01; Table 2). On the other hand, the hydrological parameters such as mean

Table 2. Pearson correlation of sediment yield with the other selected variables

	Sediment yield (t km^{-2} yr^{-1})	Area (km^2)	River Length (km)	Mean Basin Ele. (m)	Mean Temp (°C)	Mean Precipitation ($mmyr^{-1}$)	Discharge (km^3yr^{-1})	Runoff ($mmyr^{-1}$)
Sediment yield	1							
Area	0.026	1						
River Length	0.216	0.148	1					
Mean Basin Ele.	-0.009	0.583*	0.282	1				
Mean Tem	-0.478*	-0.232	0.069	-0.078	1			
Mean Precipitation	0.812**	0.282	0.508*	0.182	-0.383	1		
Runoff	0.641**	0.027	0.509*	-0.026	-0.112	0.878**	0.551*	1

* Correlation is significant at the 0.05 level; **Correlation is significant at the 0.01 level.

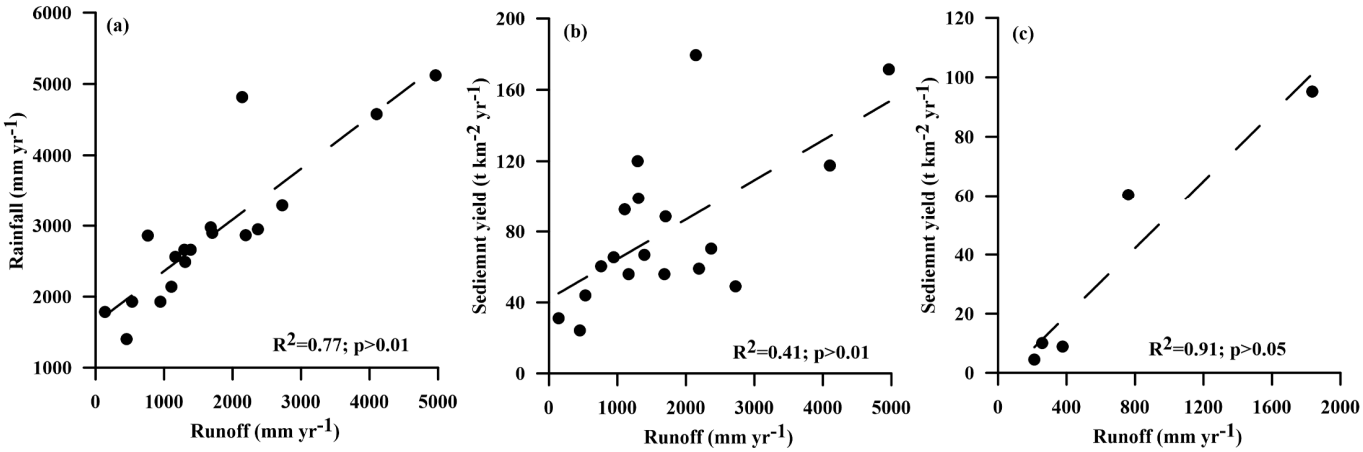

Fig.8. The correlation between **(a)** rainfall and runoff, **(b)** runoff and sediment yield of SGT region, and **(c)** runoff and sediment yield of BP river and its sub-basins.

annual precipitation and runoff showed significant (r=0.81 & r=0.64; p<0.01) positive correlations (Table 2). This preliminary analysis ruled out the parameters, which showed either negative or no relation. Further, linear regression analysis was performed on the influencing factors. The runoff pattern derived from the respective gauge stations from the rivers flowing in the SGT region mimics the pattern of rainfall (Fig. 8a; r^2=0.77; p>0.001). Therefore, the values of runoff were further used to perform quantitative relationships. The positive correlation (r^2=0.41; p>0.01) between the runoff and sediment yield in SGT catchments indicates the dominant role of runoff in basin-scale erosion (Fig.8b). This relation is even more clear for the BP river and its sub-basins (Fig. 8c; r^2=0.91; p>0.05) and validates the runoff as one of the major variables that determine the variability in sediment yield of the BP catchment.

CONCLUSION

The Bharathapuzha river flowing through the Palghat gap of the tectonically quiescent Western Ghats is the second-largest west flowing river in the Kerala state. The calculated in-situ hydrological parameters (runoff and sediment load) and derived geomorphic indices (HI, SL-index) have provided a basic understanding of the BP basin- erosion rate. The BP river is exceptional all over the WG rivers as it links the semi-arid climate in the eastern part of the WG with the humid (wet) climate in the western part of the WG. The disparity in the rainfall due to the Palghat gap, and the resultant climate change are well reflected in the discharge characteristics and suspended sediment transport of the river. The quantitative geomorphological analysis of the BP basin shows that both north and south draining sub-basins are producing high runoff and sediment flux. Among the sub-basins, the erosion rate of the Kunthipuzha basin (0.035 mm yr^{-1}) is ten times higher than the same size sub-basin (up to Ambarampalayam; 0.004 mm yr^{-1}) within the BP catchment despite draining from similar lithology. The KP basin alone contributes half of the discharge and one-fourth of sediment load out of the whole BP river basin to the Arabian Sea. The present study validates the combined influence of post-orogenic topographic steepness coupled with the strong rainfall gradient over the basin-scale erosion rate in tectonically quiescent areas.

Acknowledgments: KKR is grateful to the DST-INSPIRE fellowship program (IF150795) for financial support. HG is thankful to the University Grants Commission (UGC), New Delhi, India for an appointment, and start-up grant under Faculty Recharge Program. The Director, CSIR-National Geophysical Research Institute is acknowledged for extending necessary analytical facilities.

References

Ambili, V., Narayana, A.C. (2014) Tectonic effects on the longitudinal profiles of the Chaliyar River and its tributaries, southwest India. Geomorphology, v.217, pp.37-47.

Anderson, R.S., Anderson, S.P. (2010) Geomorphology: the mechanics and chemistry of landscapes. Cambridge University Press.

Bookhagen, B., Burbank, D.W. (2006) Topography, relief, and TRMM derived rainfall variations along the Himalaya. Geophys. Res. Lett., v.33(8), pp.1-5.

Brozoviæ, N., Burbank, D.W., Meigs, A.J. (1997) Climatic limits on landscape development in the northwestern Himalaya. Science, v.80(276), pp.571–574.

Bull, W.B. (2007) Tectonic Geomorphology of Mountains: A New Approach to Paleoseismology. Wiley-Blackwell, Oxford. 328p.

Burbank, D.W., Anderson, R.S. (2011) Tectonic geomorphology. John Wiley & Sons.

Campanile, D., Nambiar, C.G., Bishop, P., Widdowson, M., Brown, R. (2008) Sedimentation record in the Konkan–Kerala Basin: implications for the evolution of the Western Ghats and the Western Indian passive margin. Basin Res., v.20(1), pp.3-22.

Chardon, D., Jayananda, M., Chetty, T.R.K., Peucat, J.J. (2008) Precambrian continental strain and shear zone patterns: South Indian case. Jour. Geophys. Res.: Solid Earth, v.113(B8).

Chatterjee, S., Goswami, A., Scotese, C.R. (2013) The longest voyage: tectonic, magmatic, and paleoclimatic evolution of the Indian plate during its northward flight from Gondwana to Asia. Gondwana Res., v.23(1), pp.238-267.

Chen, Y.C., Sung, Q., Cheng, K.Y. (2003) Along-strike variations of morphotectonic features in the Western Foothills of Taiwan: Tectonic implications based on stream-gradient and hypsometric analysis. Geomorphology, v.56, pp.109–137.

Chetty, T.R.K., Rao, Y.B. (2006) The Cauvery shear zone, Southern Granulite Terrain, India: a crustal-scale flower structure. Gondwana Res., v.10(1-2), pp.77-85.

Collier, J.S., Sansom, V., Ishizuka, O., Taylor, R.N., Minshull, T.A., Whitmarsh, R.B. (2008) Age of Seychelles–India break-up. Earth Planet. Sci. Lett., v.272(1-2), pp.264-277.

Collins, A.S., Santosh, M., Braun, I., Clark, C. (2007) Age and sedimentary provenance of the Southern Granulites, South India: U-Th-Pb SHRIMP secondary ion mass spectrometry. Precambrian Res., v.155(1-2), pp.125-138.

Dadson, S.J., Hovius, N., Chen, H., Dade, W.B., Hsieh, M.L., Willett, S.D., Hu, J.C., Horng, M.J., Chen, M.C., Stark, C.P., Lague, D. (2003) Links between erosion, runoff variability and seismicity in the Taiwan orogen. Nature, v.426(6967), pp.648-651.

Dikshit, K.R. (2001) The Western Ghats: a geomorphic overview. Mem. Geol. Soc. India, no.47(1), pp.159-184.

Farnsworth, K.L., Milliman, J.D. (2003) Effects of climatic and anthropogenic change on small mountainous rivers: the Salinas River example. Global

Planet. Change, v.39(1-2), pp.53-64.
Ghosh, J.G., de Wit, M.J., Zartman, R.E. (2004) Age and tectonic evolution of Neoproterozoic ductile shear zones in the Southern Granulite Terrain of India, with implications for Gondwana studies. Tectonics, v.23(3), pp.1-38.
Grossman, R.L., Durran, D.R. (1984) Interaction of low-level flow with the western Ghat Mountains and offshore convection in the summer monsoon. Monthly Weather Review, v.112(4), pp.652-672.
GSI (1995) Geological survey of India's geology and minerals map of India. GSI publications, India. https://www.gsi.gov.in/.
Guha, S., Jain, V. (2020) Role of inherent geological and climatic characteristics on landscape variability in the tectonically passive Western Ghat, India. Geomorphology, v.350, pp.106840.
Gunnell, Y. (1997) Relief and climate in South Asia: the influence of the Western Ghats on the current climate pattern of peninsular India. Internat. Jour. Climatol.: Jour. Royal Meteorol. Soc., v.17(11), pp.1169-1182.
Gunnell, Y., Bourgeon, G. (1997) Soils and climatic geomorphology on the Karnataka Plateau, peninsular India. Catena, v.29(3-4), pp.239-262.
Gunnell, Y., Harbor, D.J. (2010) Butte detachment: How pre rift geological structure and drainage integration drive escarpment evolution at rifted continental margins. Earth Surface Processes and Landforms, v.35(12), pp.1373-1385.
Gunnell, Y., Gallagher, K., Carter, A., Widdowson, M., Hurford, A.J. (2003) Denudation history of the continental margin of western peninsular India since the early Mesozoic–reconciling apatite fission-track data with geomorphology. Earth Planet. Sci. Lett., v.215(1-2), pp.187-201.
Gupta, H., Kao, S.J., Dai, M. (2012) The role of mega dams in reducing sediment fluxes: A case study of large Asian rivers. Jour. Hydrol., v.464, pp.447-458.
Hack, J.T. (1973) Drainage adjustment in the Appalachians. *In* Morisawa M., (Ed.), Fluvial geomorphology: Binghamton, New York, State University of New York, pp.51–69.
Hilton, R.G., Galy, A., Hovius, N., Chen, M.C., Horng, M.J., Chen, H. (2008) Tropical-cyclone-driven erosion of the terrestrial biosphere from mountains. Nature Geoscience, v.1(11), pp.759-762.
Hooper, P.R. (1990) The timing of crustal extension and the eruption of continental flood basalts. Nature, v.345(6272), pp.246–249.
http://www.cwc.gov.in/wateryear-book
http://www.india-wris.nrsc.gov.in/
http://srtm.csi.cgiar.org/
Jaiswara, N.K., Kotluri, S.K., Pandey, A.K., Pandey, P. (2019) Transient basin as indicator of tectonic expressions in bedrock landscape: Approach based on MATLAB geomorphic tool (Transient-profiler). Geomorphology, v.346, pp.106853.
Jarvis, A., Reuter, H.I., Nelson, A., Guevara, E. (2008) Hole-filled SRTM for the globe Version 4. available from the CGIAR-CSI SRTM 90m Database (http://srtm. csi. cgiar. org) v.15, pp.25-54.
Kale, V.S., Rajaguru, S.N. (1988) Morphology and denudation chronology of the coastal and upland river basins of western Deccan Trappean landscape (India): a collation. Zeitschrift für Geomorphologie, v.32(3), pp.311-327.
Kale, V.S. (2009) The Western Ghat: the great escarpment of India. *In:* Geomorphological landscapes of the world (257-264). Springer, Dordrecht.
Kale, V.S., Vaidyanadhan, R. (2014) The Indian peninsula: geomorphic landscapes. *In:* Landscapes and landforms of India (pp. 65-78). Springer, Dordrecht.
Kao, S.J., Milliman, J.D. (2008) Water and sediment discharge from small mountainous rivers, Taiwan: The roles of lithology, episodic events, and human activities. Jour. Geol., v.116(5), pp.431-448.
Keller, E.A. (1986) Investigation of active tectonics: use of surficial earth processes. Active tectonics, v.1, pp.136-147.
Keller, E.A., Pinter, N. (2002) Active Tectonics. Earthquakes, Uplift, and Landscape. Prentice Hall, New Jersey, 362p.
Lifton, N.A., Chase, C.G. (1992) Tectonic, climatic and lithologic influences on landscape fractal dimension and hypsometry: implications for landscape evolution in the San Gabriel Mountains, California. Geomorphology, v.5(1-2), pp.77-114.
Liu, J.P., Liu, C.S., Xu, K.H., Milliman, J.D., Chiu, J.K., Kao, S.J., Lin, S.W. (2008) Flux and fate of small mountainous rivers derived sediments into the Taiwan Strait. Mar. Geol., v.256, pp.65–76.
Magesh, N.S., Jitheshlal, K.V., Chandrasekar, N., Jini, K.V. (2013) Geographical information system-based morphometric analysis of Bharathapuzha river basin, Kerala, India. Appl. Water Sci., v.3(2), pp.467-477.
Mandal, S.K., Lupker, M., Burg, J.P., Valla, P.G., Haghipour, N., Christl, M. (2015) Spatial variability of 10Be-derived erosion rates across the southern Peninsular Indian escarpment: A key to landscape evolution across passive margins. Earth Planet. Sci. Lett., v.425, pp.154-167.
Mandal, S.K., Burg, J.P., Haghipour, N. (2017) Geomorphic fluvial markers reveal transient landscape evolution in tectonically quiescent southern Peninsular India. Geol. Jour., v.52, pp.681–702.
Milliman, J.D., Syvitski, J.P. (1992) Geomorphic/tectonic control of sediment discharge to the ocean: the importance of small mountainous rivers. Jour. Geol., v.100(5), pp.525-544.
Milliman, J.D., Meade, R.H. (1983) World-wide delivery of sediment to the oceans. Jour. Geol., v.91, pp.1–21.
Milliman, J.D., Farnsworth, K.L., Albertin, C.S. (1999) Flux and fate of fluvial sediments leaving large islands in the East Indies. Jour. Sea Res., v.41, pp.97–107.
Minshull, T.A., Lane, C.I., Collier, J.S., Whitmarsh, R.B. (2008) The relationship between rifting and magmatism in the northeastern Arabian Sea. Nature Geoscience, v.1(7), pp.463-467.
Montgomery, D.R., Balco, G., Willett, S.D. (2001) Climate, tectonics, and the morphology of the Andes. Geology, v.29(7), pp.579-582.
O'Callaghan, J.F., Mark, D.M. (1984) The extraction of drainage networks from digital elevation data. Computer Vision, Graphics, and Image Processing, v.28(3), pp.323-344.
Padmalal, D., Sreelash, K., Raj, V.T., Sajan, K. (2018) River Discharge, Major Ion Chemistry and Sediment Transport of the Bharathapuzha River, Southwest India: Implications on Catchment Erosion. Jour. Geol. Soc. India, v.92(5), pp.568-578.
Pérez-Peña, J.V., Azañón, J.M., Azor, A. (2009) CalHypso: An ArcGIS extension to calculate hypsometric curves and their statistical moments. Applications to drainage basin analysis in SE Spain. Computers & Geosciences, v.35(6), pp.1214-1223.
Pérez-Peña, J.V., Azor, A., Azañón, J.M., Keller, E.A. (2010) Active tectonics in the Sierra Nevada (Betic Cordillera, SE Spain): Insights from geomorphic indexes and drainage pattern analysis. Geomorphology, v.119(1-2), pp.74-87.
Peters, G., van Balen, R.T. (2007) Tectonic geomorphology of the northern Upper Rhine graben, Germany. Global and Planetary Change, v.58(1-4), pp.310-334.
Radhakrishna, B.P. (1964) Evolution of the Sharavathy drainage, Mysore State, South India. Jour. Geol. Soc. India, v.5, pp.72-79.
Raj, N.P.P., Azeez, P.A. (2012) Trend analysis of rainfall in Bharathapuzha River basin, Kerala, India. Internat. Jour. climatol., v.32(4), pp.533-539.
Ramkumar, M., Santosh, M., Rahaman, S.M.A., Balasundareshwaran, A., Balasubramani, K., Mathew M.J., Prithiviraj, G. (2019) Tectono morphological evolution of the Cauvery, Vaigai, and Thamirabarani River basins: Implications on timing, stratigraphic markers, relative roles of intrinsic and extrinsic factors, and transience of Southern Indian landscape. Geol. Jour., v.54(5), pp.2870-2911.
Reddy, S.K.K., Gupta, H., Reddy, D.V. (2019) Dissolved inorganic carbon export by mountainous tropical rivers of the Western Ghats, India. Chem. Geol., v.530, pp.119316.
Reddy, S.K.K., Gupta, H., Badimela, U., Reddy, D.V., Kurakalva, R.M., Kumar, D. (2021) Export of particulate organic carbon by the mountainous tropical rivers of Western Ghats, India: Variations and controls. Sci. Total Environ., v.751, pp.142115.
Ruxton, B.P., McDougall, I. (1967) Denudation rates in northeast Papua from potassium-argon dating of lavas. Amer. Jour. Sci., v.265, pp.545–561.
Schumm, S.A., Schumm, S.A., Dumont, J.F., Holbrook, J.M. (2002) Active tectonics and alluvial rivers. Cambridge University Press.
Shi, X., Yang, Z., Dong, Y., Qu, H., Zhou, B., Cheng, B. (2020) Geomorphic indices and longitudinal profile of the Daba Shan, northeastern Sichuan Basin: Evidence for the late Cenozoic eastward growth of the Tibetan Plateau. Geomorphology, v.353. pp.107031.
Štìpanèíková, P., Stemberk, J., Vilímek, V., Koš,•ák, B. (2008) Neotectonic development of drainage networks in the East Sudeten Mountains and monitoring of recent fault displacements (Czech Republic). Geomorphology, v.102, pp.68–80.
Storey, B.C. (1995) The role of mantle plumes in continental break-up: case

histories from Gondwanaland. Nature, v.377(6547), pp.301-308.
Storey,, M., Mahoney, J.J., Saunders, A.D., Duncan, R.A., Kelley, S.P., Coffin, M.F. (1995) Timing of hot spot—related volcanism and the break-up of Madagascar and India. Science, v.267(5199), pp.852-855.
Strahler, A.N. (1952) Hypsometric (area-altitude) analysis of erosional topography. Geol. Soc. Amer. Bull., v.63(11), pp.1117-1142.
Thiede, R.C., Bookhagen, B., Arrowsmith, J.R., Sobel, E.R., Strecker, M.R. (2004) Climatic control on rapid exhumation along the Southern Himalayan Front. Earth Planet. Sci. Lett., v.222(3-4), pp.791-806.
Torsvik, T.H., Tucker, R.D., Ashwal, L.D., Carter, L.M., Jamtveit, B., Vidyadharan, K.T., Venkataramana, P. (2000) Late Cretaceous India–Madagascar fit and timing of break up related magmatism. Terra Nova, v.12(5), pp.220-224.
Walling, D.E., Webb, B.W. (1996) Erosion and sediment yield: A global overview. IAHS-AISH Publ. v.236, pp.3–19.
Widdowson, M., Gunnell, Y. (1999) Tertiary palaeosurfaces and lateritization of the coastal lowlands of Western Peninsula India. Palaeoweathering, Palaeosurfaces and Related Continental Deposits. International Association of Sedimentologists, Blackwell Science Ltd, Spec. Publ., v.27, pp.245-274.
Willett, S.D. (1999) Orogeny and orography: The effects of erosion on the structure of mountain belts. Jour. Geophys. Res.: Solid Earth v.104, pp.28957–28981.
Wobus, C., Whipple, K.X., Kirby, E., Snyder, N., Johnson, J., Spyropolou, K., Crosby, B., Sheehan, D. (2006) Tectonics from topography: Procedures, promise, and pitfalls. Special papers-Geol. Soc. Amer., v.398, pp.55.
Zhang, H.Y., Shi, Z.H., Fang, N.F., Guo, M.H. (2015) Linking watershed geomorphic characteristics to sediment yield: Evidence from the Loess Plateau of China. Geomorphology, v.234, pp.9–27.

(Received: 25 November 2020; Revised form accepted: 5 April 2021)

Appendix

Table A1. Time series data of annual water discharge and sediment loads from Kumbidi and Pulamanthole GD stations.

	Annual Sediment Load (10^3 t)			Annual Discharge (km^3)		
Year	Kumbidi	Pulamanthole	% Contribution	Kumbidi	Pulamanthole	% Contribution
1986-1987	0.356	0.05	12.72	3.56	1.63	45.95
1987-1988	0.155	0.05	29.20	2.70	1.05	38.76
1988-1989	0.277	0.14	49.94	4.33	1.81	41.83
1989-1990	0.301	0.11	35.96	4.12	1.64	39.70
1990-1991	0.272	0.05	19.14	3.81	1.28	33.48
1991-1992	0.576	0.12	20.70	5.54	1.82	32.79
1992-1993	0.539	0.15	28.71	6.04	2.47	40.89
1993-1994	0.354	0.07	18.86	3.69	1.50	40.75
1994-1995	0.769	0.19	25.32	6.79	2.30	33.96
1995-1996	0.371	0.09	25.57	4.74	1.73	36.45
1996-1997	0.241	0.09	35.42	3.85	1.61	41.71
1997-1998	0.333	0.12	37.20	4.04	2.01	49.62
1998-1999	0.522	0.12	22.99	5.45	2.20	40.30
1999-2000	0.281	0.08	27.95	3.61	1.89	52.32
2000-2001	0.192	0.04	22.35	2.65	1.31	49.57
2001-2002	0.290	0.09	29.82	4.23	1.62	38.43
2002-2003	0.154	0.05	35.50	2.76	1.04	37.74
2003-2004	0.088	0.03	30.70	2.14	0.78	36.30
2004-2005	0.268	0.09	33.86	3.90	1.44	37.02
2005-2006	0.334	0.13	38.60	5.58	2.13	38.13
2006-2007	0.314	0.12	36.88	6.08	2.18	35.79
2007-2008	0.571	0.23	39.76	8.40	2.79	33.25
2008-2009	0.129	0.05	40.29	2.83	1.25	44.19
2009-2010	0.389	0.11	28.49	4.91	1.81	36.78
2010-2011	0.149	0.12	77.99	5.09	2.17	42.68
2011-2012	0.405	0.10	25.94	5.74	2.24	38.97
2012-2013	0.104	0.02	18.51	2.25	0.91	40.36
2013-2014	0.289	0.05	17.90	6.01	2.08	34.57
2014-2015	0.645	0.02	2.51	6.34	2.05	32.35
2015-2016	0.211	0.01	5.38	2.85	0.94	32.94
2016-2017	0.101	0.01	12.23	1.56	0.68	43.16
2017-2018	0.199	0.04	20.31	2.99	1.48	49.48
Average	**0.318**	**0.09**	**28.34**	**4.33**	**1.68**	**39.69**

*Data obtained from CWC-Report (http://www.cwc.gov.in/sites/default/files/admin/6CWFRWYB17-18.pdf)